UDC 538.911
IRSTI 29.27.07

https://doi.org/10.55452/1998-6688-2026-23-3-448-460

[1*]Batryshev D.G.,
PhD, Associate Professor, ORCID ID: 0000-0002-9847-1067,
[*]e-mail: d.batryshev@kbtu.kz
[1,†]Abdirakhmanov A.R.,
PhD, Postdoc, ORCID ID: 0000-0001-6652-1923,
e-mail: abdirakhmanov@physics.kz
[2]Boufendi L.,
PhD, Professor, ORCID ID: 0000-0002-6995-0368,
e-mail: laifa.boufendi@physics.kz
[1,2]Orazbayev S.A.,
PhD, Associate Professor, ORCID ID: 0000-0002-7286-9990,
e-mail: sagi.orazbayev@gmail.com
[1,2]Baikaliyev A.,
PhD student, Junior researcher, ORCID ID: 0009-0000-5616-7131,
e-mail: akdauletbai@gmail.com
[1,2]Ramazanov T.S.,
Doctor of Physical and Mathematical Sciences, Professor, ORCID ID: 0000-0001-7172-8005,
e-mail: ramazan@physics.kz

[1]Kazakh-British Technical University, Almaty, Kazakhstan
[2]Al-Farabi Kazakh National University, Almaty, Kazakhstan
[†]Current address: Mons University, Mons, 7000, Belgium.

STUDY OF GROWTH EVALUATION OF NANOSTRUCTURED CARBON NITRIDE THIN LAYERS IN NITROGEN-METHANE GAS MIXTURE RADIOFREQUENCY PLASMA

Abstract

Amorphous carbon nitride (a-C_xN_y) thin films were synthesized by plasma-enhanced chemical vapor deposition (PECVD) in a nitrogen–methane radiofrequency (RF) discharge plasma (13.56 MHz) using pulsed plasma modulation. The evolution of the DC self-bias voltage (V_{dc}) was monitored as an in situ diagnostic parameter to track nanoparticle nucleation, growth, and agglomeration during synthesis. It was found that the absolute value of V_{dc} decreases monotonically following plasma ignition, and that the onset of nanoparticle agglomeration can be reliably identified from a characteristic change in the $V_{dc}(t)$ curve, consistent with the three-stage model of dust-particle formation in low-temperature plasma. The agglomeration onset time (t_{agl}) was shown to depend strongly on methane flow rate, working pressure, and RF power: at baseline conditions (0.86 mbar, 20 W), increasing the CH_4 flow rate from 2 to 7 sccm reduced t_{agl} from 4.4 s to 200 ms, while pressure and power exhibited dominant and non-monotonic effects, respectively. These findings guided the selection of plasma-on pulse durations for controlled film growth. Samples deposited under pulsed modulation were characterized by SEM, EDS, FTIR, and XRD, confirming the formation of continuous, nonstoichiometric carbon nitride films dominated by C–N and C=N bonding. The results demonstrate that self-bias voltage monitoring is an effective, accessible method for in situ control of a-C_xN_y nanoparticle growth kinetics and for tailoring film thickness, morphology, and chemical structure via pulsed RF plasma parameters.

Keywords: amorphous carbon nitride, PECVD synthesis, RF plasma, DC self-bias voltage, growth mechanism.

Received July 31, 2026; revised August 21, 2026; accepted August 26, 2026.

Introduction

Carbon nitride (CN_x) has attracted sustained research interest since theoretical calculations predicted that a hypothetical β-C_3N_4 phase could be harder than diamond. Although a phase-pure crystalline β- C_3N_4 has not yet been synthesized in continuous thin-film form, the amorphous and nanostructured carbon nitride phases obtained experimentally have proven valuable in their own right, exhibiting characteristic high resistivity, good photosensitivity, and a broad range of tunable electrical and optical properties depending on the deposition method and process conditions. These characteristics have made amorphous carbon nitride (a-CNx) attractive for protective and biomedical coatings, microelectronic devices, photosensors, solar cells, low-k dielectric materials for ULSI, and, more recently, metal-free semiconductor photocatalysts for applications such as visible-light-driven hydrogen evolution and photocatalytic hydrogen peroxide production [1].

A variety of physical and chemical vapor deposition routes have been employed to synthesize CNx thin films, each offering different control over stoichiometry, bonding structure, and morphology. Physical vapor deposition (PVD) approaches include reactive rf and dc magnetron sputtering of graphite targets in nitrogen atmospheres, reactive pulsed laser ablation, electron-beam evaporation under nitrogen-ion bombardment, and dual ion-beam-assisted sputter deposition. Chemical vapor deposition (CVD) routes, by contrast, typically rely on plasma excitation of nitrogen-containing hydrocarbon gas mixtures, including rf plasma of acetylene/nitrogen mixtures, microwave surface-wave plasma from argon/hydrocarbon/nitrogen feedstocks, and distributed electron cyclotron resonance (ECR) plasma decomposition of acetylene and nitrogen [1]. Among these, rf plasma-assisted CVD is particularly attractive owing to its relative simplicity, scalability, and the fine control it affords over plasma density, ion energy, and radical concentration through adjustable process parameters such as rf power, gas flow ratio, chamber pressure, and substrate temperature [2].

Numerous studies have shown that these plasma parameters strongly influence the resulting film microstructure. Increasing rf power raises substrate temperature, electron temperature, and plasma density within the reactor, which accelerates the deposition rate and film growth while also roughening the surface morphology, shifting it from smooth, featureless films toward cauliflower-like or broccoli-like nanostructured surfaces at higher power or longer deposition time [1, 2]. Correspondingly, optical properties such as the absorption edge, optical band gap, refractive index, and extinction coefficient vary systematically with plasma power, reflecting underlying changes in film density, polarizability, and defect concentration within the amorphous network; reported optical gaps for a-CNx films typically fall in the range of roughly 2.9–4.4 eV depending on deposition technique and nitrogen content [1]. Post-deposition plasma treatments, such as exposure to oxygen plasma, have additionally been shown to selectively etch the film surface and alter its chemical bonding state - increasing C–O bonding at the expense of C–N/C–C bonding, and in some cases inducing nitrogen-oxide species (e.g., NO_2, NO_3) at elevated deposition temperatures - with the etching rate and bonding response found to depend strongly on substrate temperature during growth. Such findings underscore that the nanostructure and surface chemistry of CNx films are highly sensitive not only to precursor chemistry but also to the specific plasma and thermal history of the film [2].

More broadly, doping and defect engineering strategies applied to conjugated carbon nitride frameworks - including nitrogen-vacancy formation, heteroatom doping, and plasma-induced structural disordering - have been shown to modulate the electronic structure, extend π-conjugation, and passivate charge-trapping states, thereby significantly influencing photophysical and photocatalytic behavior [2]. This further demonstrates that plasma-based processing is a powerful and versatile tool for tailoring the amorphous/nanostructured carbon nitride network beyond what is achievable through thermal polymerization alone [3].

Despite this substantial body of work, most rf plasma CVD studies of amorphous carbon nitride have relied on acetylene (C_2H_2) as the carbon-bearing precursor gas [1], while nitrogen–methane (N_2-CH_4) plasma systems remain comparatively less explored. Methane's simpler molecular structure, higher hydrogen-to-carbon ratio, and distinct dissociation pathway relative to acetylene may influence

radical generation, carbon–nitrogen incorporation kinetics, and the resulting film nanostructure in ways not yet systematically documented. A detailed evaluation of how growth conditions govern the structural evolution of CN_x films deposited from N_2-CH_4 rf plasma is therefore needed to establish process–structure relationships analogous to those already reported for C_2H_2-based and sputtered CNx systems [1–3].

In this work, we investigate the growth evolution of amorphous carbon nitride thin layers deposited by radiofrequency plasma in a nitrogen-methane gas mixture.

Materials and methods

The growth of amorphous carbon nitride (a-CN_x) in a high-frequency (HF) capacitive discharge plasma was studied using a plasma-enhanced chemical vapor deposition (PECVD) system, the schematic of which is shown in Figure 1.

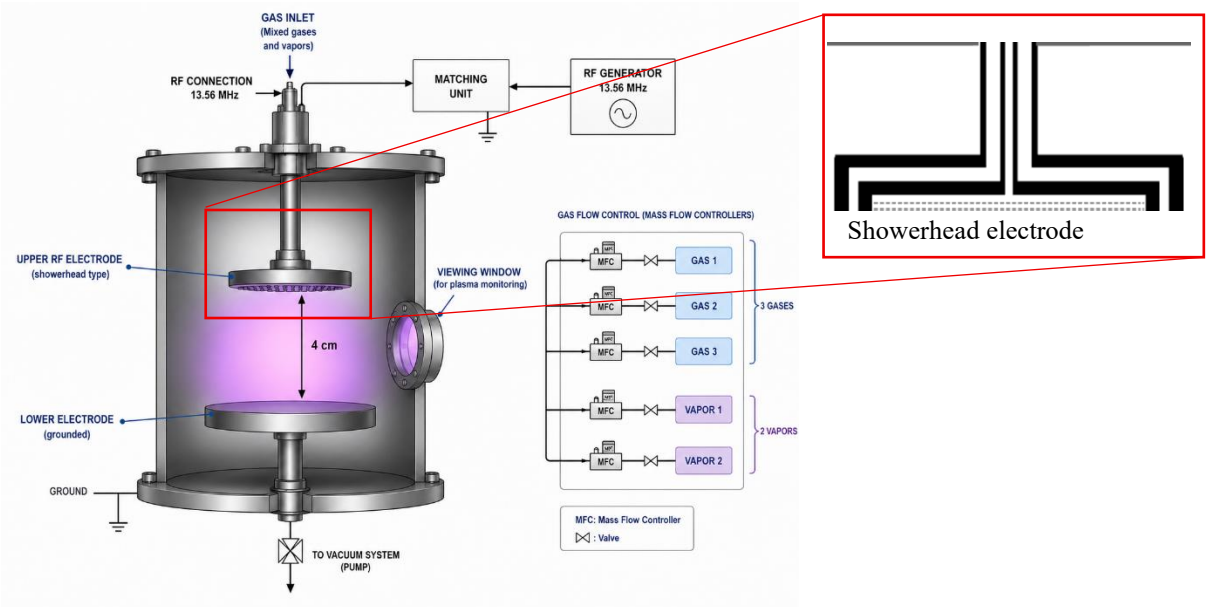

Figure 1 – Schematic of the PECVD system for nanomaterial synthesis in an RF discharge plasma

As shown in Figure 1, the plasma is formed between two plane-parallel disk electrodes upon excitation of a 13.56 MHz capacitive RF discharge through a matching network. Before each experiment, the vacuum chamber was evacuated to a residual pressure of 1.4×10^{-5} mbar, after which the working gases (Ar, N_2, CH_4) were injected into the chamber through a system of dedicated mass-flow controllers.

A distinctive feature of the developed PECVD system is the design of the upper RF electrode. It is a coaxial system with an integrated showerhead consisting of a series of holes of different diameters, which ensure uniform gas-flow distribution and laminar gas flow in the interelectrode space. The counter-electrode is grounded, similarly to the lower electrode, which promotes the formation of a bulk plasma between the electrodes and creates favorable conditions for the synthesis and confinement of nanoparticles within the plasma volume.

Because the area of the upper RF electrode is significantly smaller than the effective area of the grounded electrode (taking into account the metal walls of the vacuum chamber that are in contact with the plasma), a negative DC self-bias voltage (Vdc) developson the powered electrode due to the coupling capacitor (blocking capacitor) located in the matching box. Its formation is due to the higher mobility of electrons compared with ions, so that a negative self-bias potential appears at the electrode surface to equalize the electron and ion fluxes.

The self-bias voltage is one of the most sensitive diagnostic parameters of an RF discharge and is determined by the plasma conditions, such as discharge power, pressure, and the nature of the gas mixture. In addition, nanoparticle nucleation and growth are accompanied by changes in the free-electron concentration and charge redistribution in the plasma, which is directly reflected in the value of V_{dc}. Therefore, monitoring the evolution of the self-bias voltage during synthesis provides in situ information on the kinetics of nucleation, growth, and agglomeration of amorphous carbon nitride nanoparticles.

The self-bias voltage (DC self-bias voltage, V_{dc}) was recorded using a LeCroy PP006A high-frequency voltage probe (500 MHz bandwidth, 10:1 attenuation ratio) and a Siglent SDS5034X digital oscilloscope. A general view of the developed PECVD system and a photograph of it in operation are shown in Figure 2.

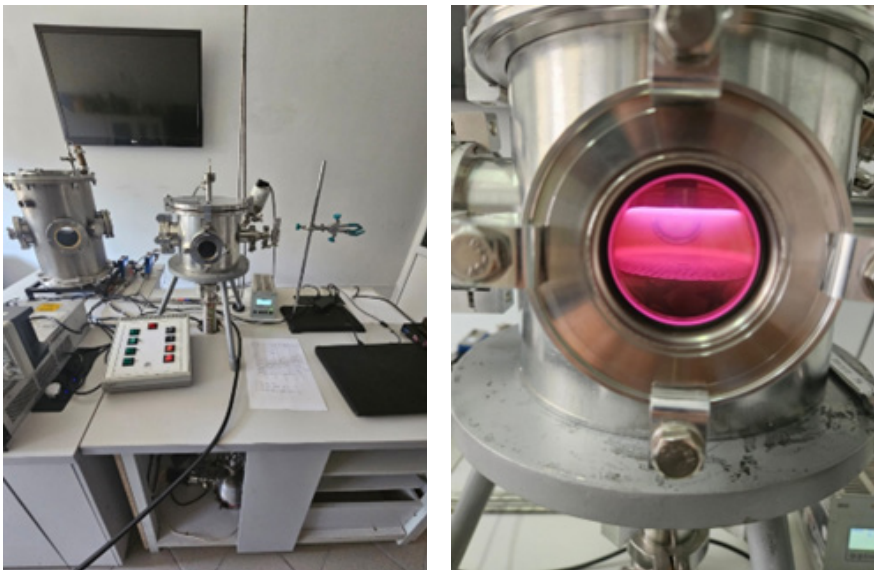

Figure 2 – General view of the PECVD system (left) and the system in operation (right)

Amorphous carbon nitride was synthesized by plasma-enhanced chemical vapor deposition (PECVD) in a nitrogen-methane plasma with pulsed RF-plasma modulation on a silicon substrate (single crystal Si (100), University Wafer, USA). The process was carried out at an RF discharge power of 20–40 W, a working pressure of 0.86–1.2 mbar, a constant nitrogen flow rate of 40 sccm, and a methane flow rate of 2–7 sccm. The modulation period was selected based on a study of the self-bias voltage evolution at different methane flow rates. After each experiment, the synthesized coatings were subjected to additional treatment in a nitrogen plasma for 10 min at an RF discharge power of 15 W. This treatment was performed to passivate surface dangling bonds, reduce the chemical reactivity of the surface, and decrease subsequent oxidation of the deposited layers in contact with the atmosphere.

The evolution of the self-bias voltage was recorded under continuous RF discharge burning in order to study the dynamics of V_{dc} during synthesis and to determine the optimal duration of plasma exposure ensuring the formation and growth of carbon nitride nanocrystals in the gas phase that will be collected on the substrate surface.

The PECVD synthesis products were deposited on silicon substrates (SiO_2). The surface morphology and elemental composition were studied by scanning electron microscopy (SEM, JSM-IT210, JEOL, Japan) with an energy-dispersive X-ray spectroscopy (EDS) system. The phase composition of the samples was determined by X-ray diffractometry (XRD, Rigaku MiniFlex 600, Rigaku, Japan), and the chemical structure and types of chemical bonds were analyzed by Fourier-transform infrared spectroscopy (FTIR, Bruker Alpha, Bruker, USA).

Results

As shown in Figure 3, immediately after plasma ignition a negative self-bias voltage of about –32 V develops at the RF electrode owing to the area asymmetry between the RF and grounded electrodes. Thereafter, the absolute value of V_{dc} gradually decreases, reflecting a change in the electron density of the plasma during nanoparticle nucleation and growth. The forming nanoparticles effectively attach electrons and get negatively charged, lowering the free-electron concentration in the plasma, which leads to a change in the self-bias potential [4, 5]. The decrease of the absolute value of V_{dc} indicates precisely the beginning of the agglomeration phase of the carbon-nitride nanocrystallites formed in the plasma gas phase [18].

An increase in the methane flow rate is accompanied by a decrease in the absolute value of Vdc and a marked reduction in the onset time of agglomeration of amorphous carbon nitride nanocrystallites. In particular, as the CH_4 flow rate is increased from 2 to 7 sccm, the agglomeration onset time decreases from 4.4 s to 200 ms, indicating faster formation and growth of carbon–nitrogen nanoparticles owing to the higher concentration of carbon-containing active radicals in the plasma.

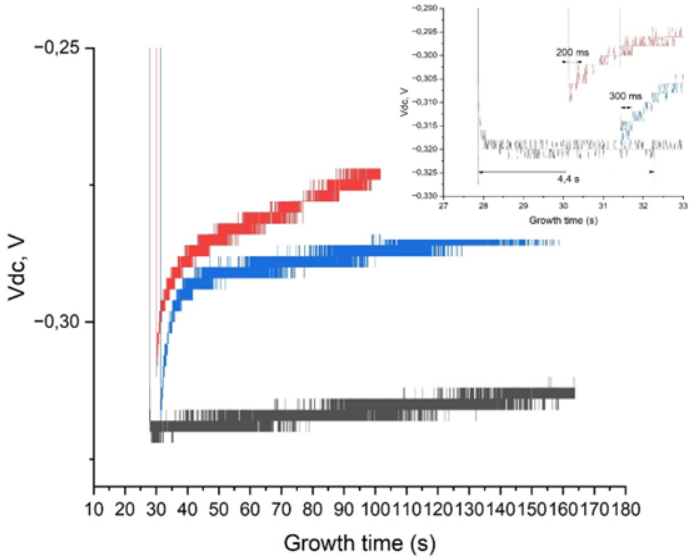

Figure 3 – Evolution of the self-bias voltage for the following plasma parameters: power 20 W, pressure 0.86 mbar, N_2 flow rate 40 sccm, CH_4 flow rate 2 (black), 5 (blue), and 7 (red) sccm. Remark: to record V_{dc} we used an attenuator between the low pass filter and the oscilloscope

Further studies of the samples obtained during the formation of amorphous carbon nitride were carried out under pulsed RF-plasma modulation, in which the plasma duration was selected according to the nanoparticle agglomeration onset time (t_{agl}). Table 1 below shows the experimental parameters, where t_{plasma_on} is the RF plasma duration, t_{plasma_off} is the duration without RF plasma, during which the synthesized products deposit on the substrate surface.

Table 1 – RF plasma modulation parameters

Sample	Power, W	Pressure, mbar	Flow rate N_2, sccm	Flow rate CH_4, sccm	Plasma modulation, ms		Number of modulation cycles
					tplasma_on	tplasma_off	
№ 1	20	0.86	40	2	4 000	2 000	2 000
№ 2				5	300		
№ 3				7	200		

Figures 4–6 show the results of surface and structural characterization of the obtained samples by scanning electron microscopy (SEM), energy-dispersive X-ray spectroscopy (EDS), Fourier-transform infrared spectroscopy (FTIR), and X-ray diffraction (XRD). According to the SEM results, a continuous thin film with uniform morphology forms on the surface of all samples after PECVD synthesis. The elemental composition of sample No. 1, determined by EDS, includes carbon (52.7 at.%), nitrogen (16.2 at.%), oxygen (3.1 at.%), and silicon (≈28 at.%), whereas the elemental composition of samples No. 2 and No. 3 is dominated by silicon (up to 100 at.%), with carbon (51.2%), nitrogen (17.2%), oxygen (11.7%), and silicon (19.9%) detected locally. The high silicon content is due to the limited thickness of the deposited film, which allows the signal from the silicon substrate to be detected. The presence of oxygen is presumably related to the formation of a thin native oxide layer on the coating surface after contact with the atmosphere. These results indicate the deposition of a nitrogen-containing carbon film on the silicon substrate.

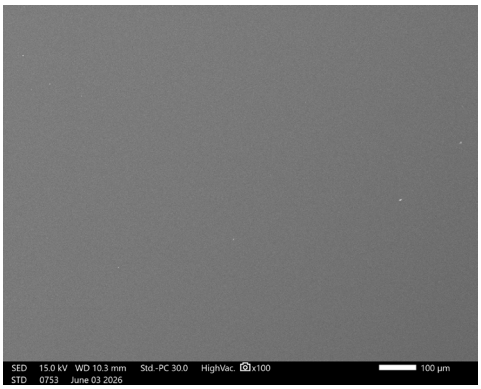

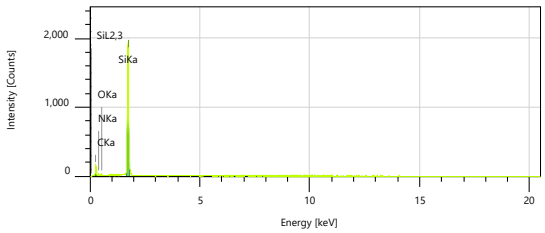

Element	Line	Mass%	Atom%
C	K	37.37±1.24	52.74±1.74
N	K	13.40±1.43	16.21±1.73
O	K	2.90±0.42	3.07±0.44
Si	K	46.34±0.79	27.97±0.48
Total		100.00	100.00

Figure 4 – SEM image of the morphology and chemical composition of the synthesized nitrogen-containing carbon film

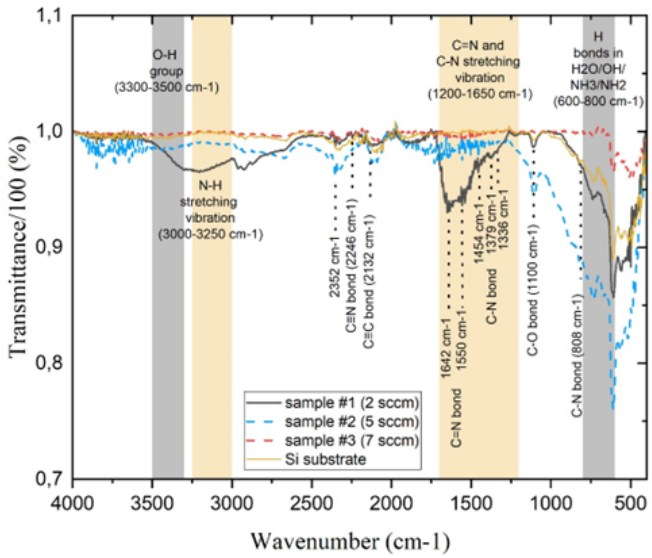

Figure 5 – FTIR spectrum of the synthesized nitrogen-containing carbon film

Figure 5 shows the FTIR spectra of the samples. In all studied samples (No. 1–No. 3), absorption bands characteristic of carbon–nitrogen compounds are observed, consistent with literature data for amorphous carbon nitride (a-C_xN_y) and polymeric C_3N_4.

The most pronounced absorption bands are observed for sample No. 1. A broad band in the 3000–3250 cm^{-1} range corresponds to N–H stretching vibrations, while the broader 3000–3500 cm^{-1} region may be associated with vibrations of N–H groups involved in hydrogen bonding, as well as with O–H groups arising from water adsorption on the coating surface [6–7].

The absorption bands at 1642 and 1550 cm^{-1} correspond to C=N stretching vibrations, while the peak at 1336 cm^{-1} can be assigned to C–N stretching vibrations linking triazine fragments with N–H groups. The bands at 1454 and 1379 cm^{-1} are also characteristic of C–N stretching vibrations in triazine rings [7–9].

Of particular interest is a weak band near 808 cm^{-1}, observed against the background of a broad band in the 500–1000 cm^{-1} range. According to the literature, this band corresponds to the breathing vibration of tri-s-triazine (heptazine) structural units, a characteristic feature of polymeric carbon nitride [10–11]. The broad band in the 600–800 cm^{-1} region may be attributed to vibrations of bonds associated with H_2O, O–H, NH_3, and NH_2 groups.

The absorption band at 2354 cm^{-1} may be related to the presence of quaternary nitrogen or adsorbed CO_2 [12], while the peak near 1100 cm^{-1} is probably due to C–O stretching vibrations.

Overall, the FTIR results indicate the formation of a nitrogen-containing carbon network dominated by C–N and C=N bonds. The set of identified absorption bands agrees with literature data for amorphous carbon nitride (a-CN_x) and suggests the possible presence of individual structural fragments of polymeric C_3N_4, in good agreement with the X-ray diffraction results (Figure 6).

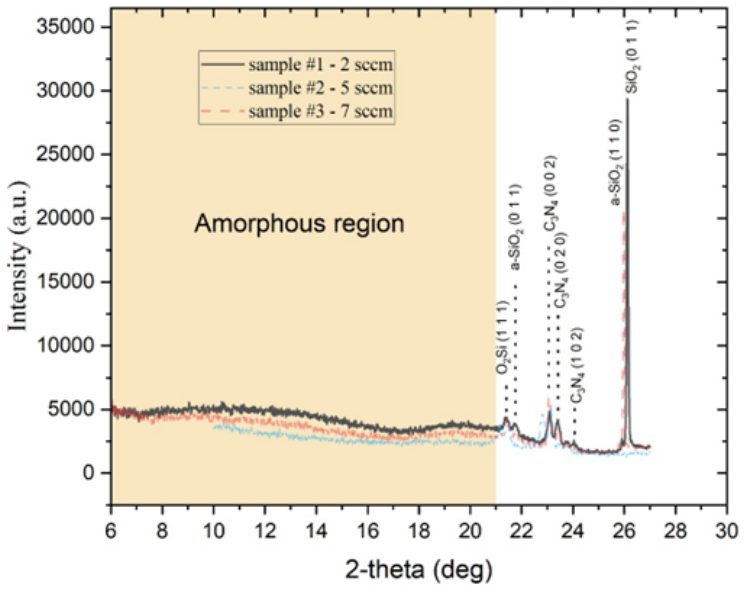

Figure 6 – XRD of synthesized a-C_3N_4 film

Figure 6 shows the X-ray diffraction results for the synthesized samples, obtained by powder X-ray diffraction over the angular range . The most intense diffraction peaks are observed for sample No. 1 and can be assigned to the C_3N_4 phase at, [13–14] and , as well as to the amorphous/crystalline SiO_2 phase at , and around . A broad diffraction maximum, characteristic of the amorphous structure of the synthesized material, is observed in the small-angle region ().

Discussion

The overall set of results obtained allows us to propose a coherent picture of the mechanism of amorphous carbon nitride (a-CNx) formation in the RF discharge plasma and to relate it to the evolution of the self-bias voltage V_{dc}.

According to the data on the temporal evolution of V_{dc} (Figure 3), a characteristic decrease in the absolute value of the self-bias voltage is observed after discharge ignition, reflecting a change in the balance of charged particles in the plasma due to nanoparticle nucleation and growth. This behavior is consistent with the three-stage model of dust-particle formation in low-temperature plasma proposed for an argon–silane discharge [4]: (i) rapid formation of nuclei – near-nanometer-sized clusters formed via chain ion–molecular reactions; (ii) coagulation of nuclei into larger agglomerates, accompanied by a sharp decrease in the free-electron concentration and, correspondingly, a change in Vdc; (iii) further particle growth via surface deposition of radicals once the acquired negative charge by the particles becomes important to stop the particle-particle agglomeration. The applicability of this model to a plasma containing carbon- and nitrogen-bearing precursors (CH_4/N_2) is confirmed by the results of V_{dc} monitoring for carbon nanoparticles under similar RF discharge conditions [5], where it was shown that the onset of particle agglomeration can be reliably identified from a characteristic kink in the $V_{dc}(t)$ curve, and that its position is sensitive to the plasma composition and parameters.

In the present work, increasing the CH_4 flow rate from 2 to 7 sccm was accompanied by a reduction in the agglomeration onset time from 4.4 s to 200 ms. This can be explained by the increased concentration of carbon-containing active species (radicals and ions) in the plasma, which increases the collision frequency and the rate of carbon–nitrogen cluster nucleation, and also accelerates the depletion of the electron component of the plasma responsible for Vdc formation [4-5]. The approach used – determining the agglomeration onset time from the Vdc evolution and then selecting the plasma-on pulse duration (t_plasma_on) for each CH_4 flow rate (Table 1) – allows the nanoparticle growth to be controllably limited at the stage preceding the agglomeration phase, yielding coatings with a more uniform morphology, as confirmed by the SEM data (Figure 4).

The EDS results indicate the formation of a carbon–nitrogen film with a C:N ratio more characteristic of nonstoichiometric amorphous carbon nitride (a-C_xN_y) in which are embedded stoichiometric C_3N_4 nanocrystallites. The presence of oxygen (3–12 at.%) in all samples is presumably related to post-growth surface oxidation upon contact with the atmosphere rather than to oxygen incorporation into the film bulk during synthesis, since after deposition the samples were additionally treated in a nitrogen plasma to passivate dangling bonds.

The FTIR data (Figure 5) confirm the formation of a carbon–nitrogen network dominated by C=N and C–N bonds, as well as the presence of the breathing vibration of tri-s-triazine (heptazine) structural units near ~808 cm^{-1} [10, 11]. Together with the bands at 1642, 1550, 1454, and 1379 cm^{-1}, assigned to triazine/heptazine ring vibrations [7–9], this points to a structural resemblance of the synthesized material to polymeric (melon- or heptazine-like) forms of carbon nitride rather than to a fully condensed crystalline C_3N_4 phase. The broad N–H and O–H bands in the 3000–3500 cm^{-1} region indicate a high degree of network disorder, the presence of terminal amino groups, and adsorbed water, typical of materials obtained by PECVD at relatively low temperatures, in contrast to high-temperature solid-state carbon nitride systems [6].

The XRD data (Figure 6) are generally consistent with this picture: the broad diffuse maximum in the small-angle region (2θ = 6–21°) reflects the predominantly amorphous structure of the film, whereas the weak peaks near $2\theta \approx$ 23–24° may be related to local ordering of carbon–nitrogen nanocrystallites. It should be noted that for graphite-like and β-C_3N_4 the characteristic (100) and (002)/(110) reflections are usually reported near $2\theta \approx$ 13° and 27–28° [13, 14], whereas the peaks observed in this work at 23–24° occupy an intermediate position; this may indicate a transitional (C_2N [15], CN [16], C_2N_3 [17]), structurally disordered phase with a shortened ordering period,

rather than a fully formed C_3N_4 crystal lattice. The presence of SiO_2 peaks ($2\theta \approx 21.4°$, 21.7°, and around 26°) is expected, since the film was synthesized on a silicon substrate with a native oxide layer, and part of the XRD signal, like the EDS signal, originates from the substrate owing to the small coating thickness.

Taken together, the SEM, EDS, FTIR, and XRD data indicate that varying the CH_4 flow rate, and the associated reduction in agglomeration time, governs not only the growth kinetics but also the final chemical structure of the synthesized material: sample No. 1 (lowest CH_4 flow rate, longest time to agglomeration) shows the most pronounced and structurally ordered FTIR bands and the most intense XRD reflections, whereas samples No. 2 and No. 3 (higher CH_4 flow rates, faster agglomeration) are characterized by a substantially smaller film thickness. This is consistent with the notion that, at high methane flow rates, rapid nucleation and coagulation of particles in the plasma bulk compete with heterogeneous deposition on the substrate, limiting the formation of a dense continuous film – an effect analogous to that described for dust particles in argon–silane and hydrocarbon plasmas [4, 5]. For example, for sample No. 1 the total synthesis time was ~2.2 h ($4s \cdot 2\,000\ cycles = 8\,000\ s$), whereas for samples No. 2 and No. 3 it was 10 min ($300\ ms \cdot 2\,000\ cycles = 600\ s$) and ~6.7 min ($200\ ms \cdot 2\,000\ cycles = 400\ s$) respectively, which fully accounts for the EDS, FTIR and XRD.

Below is a table with the results of the agglomeration onset time measurements at other RF discharge power and gas pressure values.

Table 2 – Nanoparticle agglomeration onset time (t_{agl}), determined from the evolution of the self-bias voltage V_{dc}, as a function of pressure, CH_4 flow rate, and RF discharge power (N_2 = 40 sccm)

Pressure, mbar	N_2, sccm	CH_4, sccm	t_{agl}, ms (20 W)	t_{agl}, ms (30 W)	t_{agl}, ms (40 W)
0.86	40	2	4 000	820	930
		5	300	330	500
		7	200	430	760
1		2	340	320	390
		5	360	180	350
		7	270	110	270
1.2		2	390	250	310
		5	420	170	190
		7	250	190	210

Additional measurements of t_{agl} over a wider range of pressures (0.86–1.2 mbar) and RF discharge powers (20–40 W) at a constant N_2 flow rate (40 sccm) refine the picture obtained at 0.86 mbar (Table 2). Pressure turns out to be the dominant parameter at the lowest power (20 W): already upon going from 0.86 to 1 mbar (CH_4 = 2 sccm) t_{agl} decreases by almost one order of magnitude (4000 → 340 ms), whereas a further pressure increase to 1.2 mbar changes it much less (340 → 390 ms), indicating that the nucleation process approaches saturation as the collision frequency in the plasma increases. The dependence of t_{agl} on RF discharge power, in contrast, is non-monotonic: at 0.86 mbar, increasing the power from 20 to 40 W lengthens the agglomeration onset time (for example, from 200 to 760 ms at CH_4 = 7 sccm), whereas at 1 and 1.2 mbar the minimum of t_{agl} shifts toward 30 W, followed by an increase at 40 W. This behavior can be explained by the competition between two effects of increasing power: an increase in the concentration of active carbon- and nitrogen-containing radicals, which accelerates cluster nucleation, and a simultaneous increase in gas heating and ion bombardment of the growing particles, which slows their agglomeration – an effect consistent with the independently established slowdown of nanoparticle nucleation with increasing gas temperature in RF plasma [5]. The most pronounced and monotonic sensitivity of t_{agl} to the CH_4 flow rate (an

almost twentyfold range of values) is observed precisely at 0.86 mbar and 20 W, whereas at higher pressure and power this sensitivity decreases substantially. This explains the choice of the 0.86 mbar and 20 W regime for the subsequent synthesis of the samples (Table 1): under these conditions the agglomeration onset time is most predictably governed by the methane flow rate, providing the most precise control over the pulse duration t_{plasma_on} during pulsed plasma modulation.

Conclusion

This work investigated the growth of nanostructured carbon nitride (a-C_xN_y) thin layers in an RF discharge plasma by PECVD, using the evolution of the self-bias voltage V_{dc} as an in situ diagnostic parameter. It is shown that the absolute value of V_{dc} decreases monotonically as the nanoparticles nucleate and grow in the plasma gas phase, and that the onset of their agglomeration can be reliably identified from a characteristic change in the $V_{dc}(t)$ curve, consistent with the three-stage model of dust-particle formation in low-temperature plasma.

It was found that the agglomeration onset time t_{agl} is sensitive to the plasma composition and parameters: under baseline conditions (0.86 mbar, 20 W), increasing the CH_4 flow rate from 2 to 7 sccm reduces t_{agl} from 4.4 s to 200 ms. Extended measurements over the 0.86–1.2 mbar pressure range and 20–40 W RF power range showed that pressure is the dominant parameter at low power, whereas the dependence of t_{agl} on power is non-monotonic, with a minimum near 30 W at elevated pressure. The largest and most predictable sensitivity of t_{agl} to the CH_4 flow rate is observed precisely at 0.86 mbar and 20 W, which justifies the choice of this regime for the subsequent synthesis of samples with pulsed plasma modulation, in which the plasma duration was set according to the established agglomeration onset time.

The coatings obtained under pulsed modulation are continuous thin films of nitrogen-containing carbon. According to the EDS, FTIR, and XRD data, the synthesized material corresponds to nonstoichiometric amorphous carbon nitride (a-C_xN_y) dominated by C-N and C=N bonds, in which are embedded features of tri-s-triazine (heptazine) structural fragments characteristic of polymeric forms of carbon nitride; the prominence of these features decreases systematically going from sample No. 1 (lowest CH_4 flow rate, longest time to agglomeration) to samples No. 2 and No. 3.

Thus, monitoring the evolution of the self-bias voltage is an effective and accessible method for the in situ control of the nucleation, growth, and agglomeration kinetics of a-C_xN_y nanoparticles directly during PECVD synthesis and can be used for the precise control of the thickness, morphology, and chemical structure of the resulting nitrogen-containing carbon coatings through the choice of pulsed plasma modulation parameters.

Acknowledgements

The study was carried out with the financial support of the Ministry of Science and Higher Education of the Republic of Kazakhstan (grant No AP26101409).

REFERENCES

1 Aono M., Kikuchi S., Kitazawa N., Watanabe Y. Change in surface states of amorphous carbon nitride films after exposure to oxygen plasma. Materials Science Forum. 638–642, 818–823 (2010). https://doi.org/10.4028/www.scientific.net/MSF.638-642.818

2 Mohamed S.H., El-Hossary F.M., Gamal G.A., Kahlid M.M. Optical properties of plasma deposited amorphous carbon nitride films on polymer substrates. Physica B: Physica B. 405, 254–257 (2010). https://doi.org/ 10.1016/j.physb.2009.08.069

3 Xu Q., Zheng Y., Wang S., Fu Q., Guo X., Li Y., Ren J., Cao Z., Li R., Zhao L., Huang Y. Plasma synthesis of K-doped amorphous carbon nitride with passivated trap states for enhanced photocatalytic H_2O_2 production. Journal of Alloys and Compounds. 947, 169663 (2023). https://doi.org/10.1016/j.jallcom.2023.169663.

4 Bouchoule A., Boufendi L. Particle nucleation and growth in a low-pressure argon-silane discharge. Journal Plasma Sources Science and Technology. 3, 262, (1994). https://doi.org/10.1088/0963-0252/3/3/004.

5 Orazbayev S.A., Henault M., et all. Influence of Gas Temperature on Nucleation and Growth of Dust Nanoparticles in RF Plasma. IEEE Transactions on Plasma Science. 47 (7), 3069–3073 (2019). https://doi.org/10.1109/TPS.2019.2912805.

6 Guo, X., Duan, J., Li, C., Zhang, Z. & Wang, W. Highly efficient Z-scheme gC3N4/ZnO photocatalysts constructed by co-melting-recrystallizing mixed precursors for wastewater treatment. J. Mater. Sci. 55, 2018–2031 (2020). https://doi.org/10.1007/s10853-019-04097-0

7 Yang, X., Tang, B., Wu, T. & Cao, X. g-C3N4/TiO2 composite photocatalyst and its application to asphalt for NO removal. J. Mater. Civ. Eng. 31, 04019141 (2019). https://doi.org/10.1061/%28ASCE%29MT.1943-5533.0002763

8 Li, X. et al. Synergistic effect of efficient adsorption g-C3N4/ZnO composite for photocatalytic property. J. Phys. Chem. Solids 75, 441–446 (2014). https://doi.org/10.1016/j.jpcs.2013.12.001

9 Ghafuri, H., Tajik, Z., Ghanbari, N. et al. Preparation and characterization of graphitic carbon nitride-supported l-arginine as a highly efficient and recyclable catalyst for the one-pot synthesis of condensation reactions. Sci Rep 11, 19792 (2021). https://doi.org/10.1038/s41598-021-97360-x

10 Rashidizadeh, A., Ghafuri, H., Esmaili Zand, H. R. & Goodarzi, N. Graphitic carbon nitride nanosheets covalently functionalized with biocompatible vitamin B1: synthesis, characterization, and its superior performance for synthesis of quinoxalines. ACS Omega 4(7), 12544–12554 (2019). https://doi.org/10.1021/acsomega.9b01635

11 Saravanan V., Lakshmanan P., Ramalingan C., Appl Organomet Chem 2023, 37(10), e7215. https://doi.org/10.1002/aoc.7215

12 Shcherban N.D., et. all. Melamine-derived graphitic carbon nitride as a new effective metal-free catalyst for Knoevenagel condensation of benzaldehyde with ethylcyanoacetate. Catal. Sci. Technol. (2018) 8 (11): 2928–2937. https://doi.org/10.1039/c8cy00253c

13 Thomas A., Fischer A., et. all. Graphitic carbon nitride materials: variation of structure and morphology and their use as metal-free catalysts. J. Mater. Chem., 2008, 18, 4893–4908. https://doi.org/10.1039/b800274f

14 Elamin, M.R.; Elamin, N.Y.; Ibrahim, T.G.; et. all. Facile Synthesis of β-C3N4 and Its Novel MnTeO3 Nanohybrids for Remediating Water Contaminated by Pharmaceuticals. Processes 2025, 13, 2357. https://doi.org/10.3390/pr13082357

15 Drueck U. and Kutoglu A. Experimental difference densities of hexacyanobenzene at 120 k. refinement of electron density distributions with charge-cloud models. Zeitschrift fuer Kristallographie (1979-2010), 166:233–244, 1984. https://doi.org/10.1524/zkri.1984.166.3-4.233

16 Parkes A.S. and Hughes R.E. The crystal structure of cyanogen. Acta Crystallographica. (1963). 16, 734–736. https://doi.org/10.1107/S0365110X63001924

17 A. Salamat, K. Woodhead, P.F. McMillan, R. Quesada Cabrera, A. Rahman, D. Adriaens, and F. Cora. Tetrahedrally bonded dense c2 n3 h with a defective wurtzite structure: x-ray diffraction and raman scattering results at high pressure and ambient conditions. Phys. Rev. B (2009), 80, 104106. https://doi.org/10.1103/PhysRevB.80.104106

18 Boufendi L., Gaudin J., Huet S., Viera G., Dudemaine M. Detection of particles of less than 5 nm in diameter formed in an argon–silane PECVD plasma. Applied Physics Letters. 79, 4301 (2001). https://doi.org/10.1063/1.1425431

[1*]Батрышев Д.Г.,
PhD, қауымдастырылған профессор, ORCID ID: 0000-0002-9847-1067,
*e-mail: d.batryshev@kbtu.kz
[1, †]Әбдірахманов А.Р.,
PhD, қауымдастырылған профессор, ORCID ID: 0000-0001-6652-1923,
e-mail: abdirakhmanov@physics.kz
[2]Буфенди Л.,
PhD, профессор, ORCID ID: 0000-0002-6995-0368,
e-mail: laifa.boufendi@physics.kz
[1,2]Оразбаев С.А.,
PhD, қауымдастырылған профессор, ORCID ID: 0000-0002-7286-9990,
e-mail: sagi.orazbayev@gmail.com
[1,2]Байқалиев А.,
докторант, МНС, ORCID ID: 0009-0000-5616-7131,
e-mail: akdauletbai@gmail.com
[1,2]Рамазанов Т.С.,
ф.-м.ғ.д., профессор, ORCID ID: 0000-0001-7172-8005,
e-mail: ramazan@physics.kz

[1]Қазақстан-Британ техникалық университеті, Алматы қ., Қазақстан
[2]Әл-Фараби атындағы Қазақ ұлттық университеті, Алматы қ., Қазақстан
†Қазіргі мекенжайы: Монс университеті, Монс қ., Бельгия

АЗОТ–МЕТАН ГАЗ ҚОСПАСЫНЫҢ РАДИОЖИІЛІКТІ ПЛАЗМАСЫНДА КӨМІРТЕК НИТРИДІНІҢ НАНОҚҰРЫЛЫМДЫ ЖҰҚА ҚАБАТТАРЫНЫҢ ӨСУ ПРОЦЕСІН ЗЕРТТЕУ

Андатпа

Аморфты көміртек нитридінің (a-CN_x) жұқа қабықшалары плазманы импульстік модуляциялау режимін қолдана отырып, 13,56 МГц жиіліктегі азот-метан газ қоспасының радиожиілікті (РЖ) разряд плазмасында плазмамен белсендірілген химиялық бу фазасынан тұндыру (PECVD) әдісімен синтезделді. Тұрақты өздігінен ығысу кернеуінің (V_{dc}) динамикасы нанобөлшектердің нуклеациясын, өсуін және агломерациясын тікелей синтез үдерісі барысында бақылау үшін диагностикалық параметр ретінде тіркелді. Плазма тұтанғаннан кейін V_{dc} абсолюттік мәнінің монотонды түрде төмендейтіні анықталды. Нанобөлшектер агломерациясының басталуын $V_{dc}(t)$ тәуелділігінің сипатты өзгерісі бойынша анықтауға болады. Бұл нәтиже төмен температуралы плазмада тозаңды бөлшектерінің түзілуінің үш сатылы моделімен сәйкес келеді. Агломерацияның басталу уақыты (t_{agl}) метан шығынына, жұмыс қысымына және РЖ-разряд қуатына айтарлықтай тәуелді екені көрсетілді. Қалыпты жағдайларда (0,86 мбар, 20 Вт) CH_4 шығынын 2-ден 7 sccm-ге дейін арттыру t_{agl} мәнін 4,4 с-тан 200 мс-қа дейін қысқартады, ал қысым мен қуаттың әсері сәйкесінше басым және монотонды емес сипатқа ие. Алынған нәтижелер қабықшалардың бақыланатын өсуі кезінде плазманың қосылу импульсінің оңтайлы ұзақтығын таңдау үшін пайдаланылды. Импульстік модуляция режимінде тұндырылған үлгілер SEM, EDS, FTIR және XRD әдістерімен зерттелді. Зерттеу нәтижелері құрамында C–N және C=N байланыстары басым болатын тұтас стехиометриялық емес көміртек нитриді қабықшаларының түзілгенін растады. Алынған нәтижелер өздігінен ығысу кернеуін бақылау a-CN_x нанобөлшектерінің өсу кинетикасын тікелей синтез үдерісі барысында қадағалаудың тиімді әрі қолжетімді әдісі екенін көрсетеді. Сонымен қатар, импульстік РЖ-плазма параметрлерін өзгерту арқылы қабықшалардың өсуін, морфологиясын және химиялық құрылымын басқаруға мүмкіндік береді.

Түйін сөздер: аморфты көміртек нитриді, PECVD синтезі, радиожиілікті плазма, тұрақты өздігінен ығысу кернеуі (DC self-bias), өсу механизмі.

[1*]Батрышев Д.Г.
PhD, ассоциированный профессор, ORCID ID: 0000-0002-9847-1067,
*e-mail: d.batryshev@kbtu.kz
[1, †]Әбдірахманов А.Р.
PhD, ассоциированный профессор, ORCID ID: 0000-0001-6652-1923,
e-mail: abdirakhmanov@physics.kz
[2]Буфенди Л.
PhD, профессор, ORCID ID: 0000-0002-6995-0368,
e-mail: laifa.boufendi@physics.kz
[1,2]Оразбаев С.А.
PhD, ассоциированный профессор, ORCID ID: 0000-0002-7286-9990,
e-mail: sagi.orazbayev@gmail.com
[1,2]Байқалиев А.,
PhD студент, МНС, ORCID ID: 0009-0000-5616-7131,
e-mail: akdauletbai@gmail.com
[1,2]Рамазанов Т.С.,
д.ф.-м.н., профессор, ORCID ID: 0000-0001-7172-8005,
e-mail: ramazan@physics.kz

[1]Казахстанско-Британский технический университет, г. Алматы, Казахстан
[2]Казахский национальный университет им. аль-Фараби, г. Алматы, Казахстан
[†]Текущий адрес: Университет Монса, г. Монс, Бельгия

ИССЛЕДОВАНИЕ ПРОЦЕССА РОСТА НАНОСТРУКТУРИРОВАННЫХ ТОНКИХ СЛОЕВ НИТРИДА УГЛЕРОДА В РАДИОЧАСТОТНОЙ ПЛАЗМЕ ГАЗОВОЙ СМЕСИ АЗОТ-МЕТАН

Аннотация

Аморфные тонкие пленки нитрида углерода (a-CN_x) были синтезированы методом плазменно-активированного химического осаждения из газовой фазы (PECVD) в радиочастотной (РЧ) разрядной плазме азотно-метановой газовой смеси при частоте 13,56 МГц с использованием импульсной модуляции плазмы. Динамика постоянного напряжения автосмещения (V_{dc}) регистрировалась в качестве диагностического параметра непосредственно в процессе синтеза для мониторинга зародышеобразования, роста и агломерации наночастиц. Установлено, что после зажигания плазмы абсолютное значение V_{dc} монотонно уменьшается, а начало агломерации наночастиц может быть достоверно определено по характерному изменению зависимости $V_{dc}(t)$, что согласуется с трехстадийной моделью формирования пылевых частиц в низкотемпературной плазме. Показано, что время начала агломерации (t_{agl}) существенно зависит от расхода метана, рабочего давления и мощности ВЧ-разряда: при базовых условиях (0,86 мбар, 20 Вт) увеличение расхода CH_4 с 2 до 7 sccm сокращает t_{agl} с 4,4 с до 200 мс, тогда как влияние давления и мощности характеризуется соответственно доминирующим и немонотонным характером. Полученные результаты использованы для выбора продолжительности импульсов включения плазмы при контролируемом росте пленок. Образцы, осажденные в режиме импульсной модуляции, исследованы методами SEM, EDS, FTIR и XRD, что подтвердило формирование сплошных нестехиометрических пленок нитрида углерода с преобладанием связей C–N и C=N. Полученные результаты показывают, что мониторинг напряжения автосмещения является эффективным и доступным методом контроля кинетики роста наночастиц a-CN_x непосредственно в процессе синтеза, а также позволяет регулировать рост, морфологию и химическую структуру пленок посредством параметров импульсной ВЧ-плазмы.

Ключевые слова: аморфный нитрид углерода, PECVD синтез, радиочастотная плазма, DC самосмещения, механизм роста.